The C−H Stretch Intensities of Polycyclic Aromatic Hydrocarbon Cations. Origins and Astrophysical Implications

Timothy W. Schmidt,*,†,§ Thomas Pino,‡ and Philippe Bréchignac‡

School of Chemistry, The University of Sydney, NSW 2006, Australia, and Laboratoire de Photophysique Moléculaire, CNRS, UPR-3361, bâtiment 210, Université Paris-Sud, F-91405 Orsay, France

Received: February 1, 2009; Revised Manuscript Received: March 1, 2009

Infrared vibrational transition intensities of polycyclic aromatic hydrocarbons are known to depend strongly on the charge state. The detailed understanding of this effect for the C−H stretching modes has been approached by applying the quantum theory of atoms in molecules. Several benchmark calculations were undertaken in order to disentangle charge and size effects, from benzene (C_6H_6) up to the ovalene ($C_{32}H_{14}$) molecule. Upon decomposition of the dipole moment derivative along a C−H stretch into charge, charge flux, and dipole flux terms, it is found that it is the competition between the sum of the first two terms and the latter which drives the intensity, due to their opposing signs. Additionally, while the dipole flux term changes very little with size and charge, the other terms are strongly sensitive to these. This effect leads to a very weak C−H stretch intensity for cation sizes close to pyrene ($C_{16}H_{10}$) and comparable intensities between neutral and cations for the much larger ones. The astrophysical implications are discussed.

Introduction

Polycyclic aromatic hydrocarbons (PAHs) form a class of molecules covering a broad range of interests due to their widespread distribution on Earth, either naturally occurring, as byproducts of natural processes, such as combustion, or as byproducts of human activities. They are also widely believed to be abundant in Space.[1] In particular, they are considered to be the carrier of a ubiquitous set of infrared emission features,[2,3] known as the aromatic infrared bands (AIBs), observed in many astrophysical objects since the early 1970s.[4] Indeed, the AIBs are well modeled as a superposition of various PAH spectra.[5] The strongest AIBs lie at 3.3, 6.2, 7.7, 8.6, 11.3, and 12.4 μm, there being some additional weaker features.[6,7] Because of the coincidence of the positions with the infrared active normal mode positions in aromatic material[8] and because of the constraint of the excitation mechanism which points to a molecular size rather than a solid, these were postulated to originate from PAHs.[2,3]

After absorption of a single starlight UV photon through an electronic transition, internal conversion (IC) takes place on a rapid time scale ($\lesssim$picoseconds), progressively degrading the electronic energy into vibrational energy on the electronic ground state. Each IC event ($S_n \rightarrow S_{n-1}$) is followed by intramolecular vibrational redistribution. This energy redistribution process, easily accomplished by PAHs, is called the *transient heating mechanism*, which allows vibrational fluorescence through the above cited bands even though the equilibrium temperature of the observed interstellar region is much colder, i.e., a few tens of kelvin. These bands can carry up to 40% of the infrared luminosity of a galaxy, and the carriers should contain about 20% of the cosmic carbon.[1] Unfortunately, the detailed knowledge of the structure and distribution of the carriers has so far escaped identification.

Thanks to dedicated observations, the AIBs have been shown to be ubiquitous in our galaxy and other galaxies. In particular, the whole spectrum has been found to be extremely stable in shape in most sources,[9,10] which implies that the mean size distribution of PAHs and their charge states are quite stable. In fact, a fundamental property of these molecules is the charge state dependence of their infrared intensities. They have been shown to exhibit strong C−H stretching modes and out-of-plane wagging motions while neutral. In their cationic state, the C−C stretches and in-plane bending modes are strongly enhanced while the C−H stretches are much weaker, at least for smaller PAHs. This property has appeared to be extremely useful in interpreting the intensity variations in some astronomical objects[10,11] and is now widely used to probe the physical conditions of the region under scrutiny. The variation in C−C to C−H intensity is correlated to the local UV flux and remains at present the best way to use the AIBs as a probe,[11,12] apart from their positive detection. It should be mentioned that the AIBs have been previously classified into three families that seem to trace different evolutionary stages of the carbonaceous interstellar dust,[9,13−15] and that the so-called class A is the dominant one by far. The carriers of the class A AIBs are those expected to be close to PAHs, having a few tens of carbon atoms up to few hundreds according to various models.[1,12,16,17]

The charge state effect on the relative intensity of the C−C and C−H stretching features has been observed experimentally on all measured PAHs.[18−22] Quantum chemical calculations also predicted this effect and revealed that it is truly specific to the positive charge.[23−34] It should be noted that anionic PAHs are predicted to be intermediate between the neutral and cationic states.[24] However, the collapse of the C−H intensities is predicted to be size dependent in favor of recent calculations on larger PAHs, while the other in-plane modes do not exhibit such a strong size dependence.[30,32−34] The small anionic PAHs have very low C−H stretch intensities and, as the size increases, the C−H stretch gains intensity toward the neutral value. A size-dependent behavior seems to proceed in the dications as well, but the C−H collapse happens at larger sizes than in the

* Corresponding author, t.schmidt@chem.usyd.edu.au.
† School of Chemistry, The University of Sydney.
‡ Laboratoire de Photophysique Moléculaire, associé à l'Université Paris XI et à la Fédération de recherche Lumière Matière.
§ Visiting Laboratoire de Photophysique Moléculaire.

10.1021/jp900931e CCC: $40.75
Published on Web 03/25/2009

cations.[32,35] Although it is now a clear property, no definitive explanation has yet been found. When calculated using different quantum chemical methods, it appears that the charge distribution difference between the neutral and the cation do not shed light on a clear mechanism.[30,31]

In light of dedicated work on infrared intensities of the C−H stretching modes in hydrocarbons, we present here an explanation of the behavior of the PAH family of molecules. The paper is organized as follows. In the second section we present an analysis of infrared intensities within the frame of the quantum theory of atoms in molecules. In the third section we present the computational details, and in the fourth section the results are given on a set of representative PAHs, with the emphasis on benzene as the prototype aromatic molecule. In the last section we then discuss the results and their astrophysical implications.

The Intensity of Vibrational Transitions

Under the adiabatic Born−Oppenheimer approximation, the intensity of a purely vibrational transition may be computed by evaluating the integral

$$M = \int \Phi'(\mathbf{Q})\mu(\mathbf{Q})\Phi''(\mathbf{Q})\,\mathrm{d}\mathbf{Q} \tag{1}$$

where $\mathbf{Q}$ are the internal normal coordinates of the molecule and $\mu(\mathbf{Q})$ is the geometry-dependent molecular dipole moment, calculated by integrating over the electronic wave function. In the harmonic approximation, the vibrational wave functions may be written as a product of harmonic oscillator eigenfunctions, $\phi_i^{v_i}(Q_i)$, with v_i quanta in mode i

$$\Phi(\mathbf{Q}, \{v_i\}) = \prod_i \phi_i^{v_i}(Q_i) \tag{2}$$

By expanding the geometry-dependent molecular dipole moment as a Taylor series in the internal normal coordinates, we obtain

$$\mu(\mathbf{Q}) = \mu_0 + \sum_i Q_i \frac{\partial \mu}{\partial Q_i} + \ldots \tag{3}$$

Experimentally one is usually interested in the intensity of transitions from the molecular ground state, ($\{v_i = 0\}$), to one in which one quantum of vibration is populated in a particular mode, $v_j = 1$. Equivalently, in emission, from a state where one mode is populated with n quanta to a state where there is one less quantum in that mode. In the case of emission from $v_j = 1$ to 0, eq 1 reduces to

$$M_j^{1-0} = \frac{\partial \mu}{\partial Q_j} \int \phi_j^{1}(Q_j) Q_j \phi_j^{0}(Q_j)\,\mathrm{d}Q_j$$

$$= \frac{\partial \mu}{\partial Q_j} \frac{1}{\sqrt{2 m_j \omega_j}} \tag{4}$$

in atomic units, where m_j is the reduced mass and ω_j is the angular frequency of mode j. As such, for a given frequency and reduced mass, the transition dipole moment, M, of a vibrational transition from the ground state to one quantum in any mode is proportional to the derivative of the molecular dipole moment with respect to that mode.

In absorption, the rate of population of the upper state, $|\Phi'\rangle$, is proportional to the square of the transition dipole moment M_j^{1-0}

$$|M_j^{1-0}|^2 = \left(\frac{\partial \mu}{\partial Q_j}\right)^2 \frac{1}{2 m_j \omega_j} \tag{5}$$

The oscillator strength is proportional to this quantity multiplied by the energy of the transition ($\hbar\omega_j$) which is thus proportional to the square of the dipole derivative divided by the reduced mass of the oscillator. Infrared intensities are usually quoted as

$$I_j^{1-0} = \left(\frac{\partial \mu}{\partial Q_j}\right)^2 \frac{1}{m_j} \tag{6}$$

with units of $\mathrm{D^2\ Å^{-2}\ amu^{-1}}$ ($1\ \mathrm{D^2\ Å^{-2}\ amu^{-1}} = 42.26\ \mathrm{km\ mol^{-1}}$).

The derivative of the molecular dipole moment can be partitioned in various ways. If the charge distribution is described as a set of point charges q_i at positions $\mathbf{r}_i$

$$\boldsymbol{\mu} = \sum_i \boldsymbol{r}_i q_i(\boldsymbol{r}_i)$$

$$\mathrm{d}\boldsymbol{\mu} = \sum_i \mathrm{d}\boldsymbol{r}_i q_i(\boldsymbol{r}_i) + \sum_i \boldsymbol{r}_i\,\mathrm{d}q_i(\boldsymbol{r}_i) \tag{7}$$

The first term is the *charge* contribution while the second represents the change in charge distribution and is referred to as *charge flux*. Such a decomposition of the dipole moment derivative is called "charge−charge flux" (CCF).

Alternatively, if the charge distribution is represented as a sum of point charges and dipoles, then

$$\begin{aligned}
\boldsymbol{\mu} &= \sum_i \boldsymbol{r}_i q_i(\boldsymbol{r}_i) + \sum_i \boldsymbol{\mu}_i(\boldsymbol{r}_i) \\
\mathrm{d}\boldsymbol{\mu} &= \sum_i \mathrm{d}\boldsymbol{r}_i q_i(\boldsymbol{r}_i) + \sum_i \boldsymbol{r}_i\,\mathrm{d}q_i(\boldsymbol{r}_i) + \sum_i \mathrm{d}\mu_i(\boldsymbol{r}_i) \\
\frac{\mathrm{d}\boldsymbol{\mu}}{\mathrm{d}Q} &= \sum_i \frac{\mathrm{d}\boldsymbol{r}_i}{\mathrm{d}Q} q_i(\boldsymbol{r}_i) + \sum_i \boldsymbol{r}_i \frac{\mathrm{d}q_i(\boldsymbol{r}_i)}{\mathrm{d}Q} + \sum_i \frac{\mathrm{d}\boldsymbol{\mu}_i(\boldsymbol{r}_i)}{\mathrm{d}Q} \\
&= C + CF + DF
\end{aligned} \tag{8}$$

In this case the dipole moment change can be decomposed into charge (C), charge flux (CF), and dipole flux terms (DF), abbreviated as CCFDF.[36−39]

Application of this procedure requires a description of the charge distribution. Popular decompositions of the charge density such as the Mulliken or Löwdin charges are unsatisfactory due to their dependence on the basis set description of the electronic wave function. Specifically, these descriptions suffer from components of the charge distribution due to a particular basis function centered on a particular nucleus being attributed to that nucleus, even far from it, or even closer to another nucleus. A description of the charge density is required which is derived directly from the calculated density itself, without regard to the one-electron basis used in the calculation. Inherent in the idea of decomposing the charge distribution into contributions from points in space is the concept of *atoms in molecules*.[40−42]

In the *quantum theory of atoms in molecules* (QTAIM) approach, a delineation of the 3-space of the molecule is made whereby boundaries between atoms are defined by the derivatives of the electronic density, ρ. Surfaces $S(\boldsymbol{r}_s)$ defined by $\nabla\rho(\boldsymbol{r}_s)\cdot\boldsymbol{n}(\boldsymbol{r}_s) = 0$, where $\boldsymbol{n}(\boldsymbol{r}_s)$ is the surface normal, form boundaries between the regions of electron density, V_i. The integrated charge q_i within this region is attributed to the point $\boldsymbol{r}_i$, defined by the local maximum in the electronic density near the associated nucleus, termed the *attractor*. A dipole $\boldsymbol{\mu}_i$ placed at the attractor $\boldsymbol{r}_i$ accounts for any discrepancy between the center of charge and the attractor. Such a distribution of charges and dipoles reproduces the molecular dipole moment and is independent of method of calculation and choice of basis set so long as the method chosen provides an adequate description of the true electron density. The QTAIM method is thus well suited to a CCFDF decomposition of the dipole moment derivative. A detailed description of the QTAIM may be found in refs 41 and 42.

The dipole derivatives of normal modes of vibration are calculated by multiplication of the normal mode vector described in the laboratory Cartesian frame by the atomic polar tensor (APT)

$$\mathbf{P} = \begin{pmatrix} \frac{\partial\mu_x}{\partial x} & \frac{\partial\mu_x}{\partial y} & \frac{\partial\mu_x}{\partial z} \\ \frac{\partial\mu_y}{\partial x} & \frac{\partial\mu_y}{\partial y} & \frac{\partial\mu_y}{\partial z} \\ \frac{\partial\mu_z}{\partial x} & \frac{\partial\mu_z}{\partial y} & \frac{\partial\mu_z}{\partial z} \end{pmatrix} \tag{9}$$

In the spirit of QTAIM, each atom's contribution to the dipole moment derivative of a particular mode of vibration may be evaluated by inspection of the APT. This may be decomposed into the CCFDF terms by performing QTAIM calculations at neighboring geometries related by a displacement along a particular coordinate. What is more, since the calculated intensities of vibrational normal modes follow linear algebra, the essence of the dipole moment derivative for a hydrogen stretch or wagging motion is embodied in the APT element for that atom, assuming that other atoms only move negligibly.

Before moving further, it is helpful to recall that a normal mode can be expressed as a linear combination of local modes, as both may be considered as linear combinations of the Cartesian displacements of each atom. Furthermore, it is possible to perform a rotation of the Cartesian basis of atomic vibrations such that each hydrogen atom's vibrations are described in terms of any three orthonormal vectors, not necessarily parallel to the Cartesian axes. If one if these is parallel to the C−H bond axis, then it follows that the C−H stretch normal modes will be dominated by the APT elements corresponding to these displacement vectors. It is thus only necessary to consider the individual APT elements parallel to the C−H bond axis in exploring the CCFDF decomposition of, and the effect of ionization on, the C−H stretch intensities. In the following, we explicitly consider only local modes of vibration, with the understanding that the conclusions are also valid for the normal modes of vibration.

Computational Details

Initial exploration of basis set dependencies of the APT were performed using PC GAMESS version 7.1, based on the GAMESS suite of electronic structure programs.[43,44] Equilibrium geometries and harmonic frequencies were calculated using density functional theory employing the B3LYP functional (LYP + VWN1 correlation). Calculations on open-shell systems were of the unrestricted type.

Numerical dipole moment derivatives were obtained by performing AIM calculations using the GAUSSIAN 03 suite of electronic structure programs.[45] The dipole moment derivative of each C−H bond elongation was obtained by executing single point calculations at the equilibrium geometry and at a displacement along the C−H stretching coordinate (typically 0.01 Å). The QTAIM decomposition of the dipole moment derivative was thus calculated by summing over the attractors

$$C = \sum_i \frac{\Delta\boldsymbol{r}_i}{\Delta Q} q_i(\boldsymbol{r}_i) \tag{10}$$

$$CF = \sum_i \boldsymbol{r}_i \frac{\Delta q_i(\boldsymbol{r}_i)}{\Delta Q} \tag{11}$$

$$DF = \sum_i \frac{\Delta\boldsymbol{\mu}_i(\boldsymbol{r}_i)}{\Delta Q} \tag{12}$$

TABLE 1: Atomic Polar Tensor (APT) Elements for Hydrogen in Neutral Benzene (Units in D/Å)[a]

method	basis	$\partial\mu_x/\partial x$	$\partial\mu_y/\partial y$	$\partial\mu_z/\partial z$
B3LYP	4-31G	0.300	−0.647	0.594
	6-31G	0.306	−0.635	0.614
	6-31G(d)	0.273	−0.610	0.535
	6-31G(d,p)	0.275	−0.578	0.523
	6-311G(d)	0.326	−0.656	0.659
	6-311+G	0.341	−0.649	0.737
	6-311+G(d,p)	0.323	−0.527	0.677
MP2	6-31G(d)	0.323	−0.677	0.628
	6-31G(d,p)	0.332	−0.635	0.621
	6-311G(d)	0.354	−0.606	0.685
	6-311+G	0.343	−0.715	0.797
	6-311+G(d,p)	0.345	−0.574	0.740
CCSD	6-31G(d)	0.303	−0.549	0.598
	6-31G(d,p)	0.264	−0.576	0.558

[a] The hydrogen lies on the positive part of the *y*-axis with the D_{6h} symmetry axis being the *z*-axis.

Results

Benzene. As the prototypical aromatic molecule, one would expect benzene to exhibit the properties exhibited by larger PAHs with regard to the intensities of vibrational transitions. While it has been shown before that basis sets as small as 4-31G can be used reliably to predict trends with regard to vibrational intensities,[24] we verified this by calculating the atomic polar tensor elements with a range of Gaussian basis sets and methods. The results are given in Table 1. All basis sets employed are seen to predict similar APT elements for neutral benzene, though those without polarization functions appear as outliers, as might be expected. The trend with increasing basis set quality is generally toward smaller absolute values of the APT elements. Importantly, the B3LYP method performs very similarly to CCSD with the moderate basis set sizes employed. Due to its widespread use and applicability to large molecules, we employed the B3LYP/6-31G(d) method for the remainder of our calculations. The APT elements listed in Table 1 demonstrate that, for the in-plane and out-of-plane bending modes of the hydrogen, the dipole moment follows the displacement of the hydrogen, with the out-of-plane vibration being the more

TABLE 2: Numerical QTAIM Decomposition of the APT Elements for the C−H Stretch of Benzene (Units in D/Å)

component	neutral	cation	Δ
C	+0.181	+0.677	+0.497
CF	+0.744	+1.348	+0.604
DF	−1.563	−1.643	−0.080
total	−0.638	+0.383	+1.021

intense. This effect has been investigated in terms of a rehybridization moment of the carbon atom.[46,47] Nevertheless, these vibrations are consistent with the idea of a vibrating point charge of about $+0.06e$ for the in-plane vibrations and $+0.11e$ for the out-of-plane vibrations. This accords well with the Mulliken and Löwdin charges calculated for the hydrogen, which are in this range. However, it is seen that the APT element for the C−H stretching mode is negative. Indeed, it has been shown that the sp_2 and sp_3 C−H stretching modes of all neutral hydrocarbons show this property.[48]

Understanding the negative APT element for the C−H stretch requires a decomposition of the contributions to the dipole moment change effected upon elongation of the C−H bond. In terms of the quantum theory of atoms in molecules (QTAIM), the dipole moment change is partitioned into three contributions: the charge (*C*), the charge flux (*CF*) and the dipole flux (*DF*). This decomposition is given in Table 2. As expected, the charge contribution is positive, reflecting the integral of the charge density within the portion said to "belong" to the hydrogen ($+0.036e$ for the neutral) in the QTAIM approach. Interestingly, the *CF* term is also large and very positive, due to an electron stripping of the hydrogen. The adjoining carbon increases its total electron density by more than this, but the contribution to the molecular dipole is less due to its greater proximity to the center of the molecule. While these two contributions to the dipole nearly cancel, the total is in favor of a positive dipole moment.

While the charge movements across atomic boundaries account for the *CF* term, if an electron density packet moves only "just" across the boundary, this *CF* term will be nearly all canceled by the *DF* term, which accounts for the displacement of the center-of-charge of each atom-in-molecule from its attractor. In the case of neutral benzene, the *DF* term is large and negative. Indeed, it is large enough to overcome the *C* and *CF* terms and results in a total negative dipole derivative. Analysis of the *DF* term atom-by-atom reveals that it is dominated by a negative dipole moment change on the carbon atom adjoining the displaced hydrogen. This indicates that the electron density stripped from the hydrogen moves across the boundary between the atoms, but not as far as the carbon attractor. Additional electron density flowing into the carbon does not cancel the dipole moment. The sum of the QTAIM terms is slightly different from the analytical result in Table 1. The 5% discrepancy is accounted for by a 2% difference due to the finite displacement of the hydrogen (0.01 Å) and a 3% error due to the numerical errors associated with the decomposition. Nevertheless, these errors are small compared to the differences between basis sets and, undoubtedly, between DFT and reality.

Upon ionization, benzene suffers Jahn−Teller distortion and thus loses the equivalence between hydrogens.[49] The molecule undergoes a transition from D_{6h} symmetry to the lower D_{2h} point group. The results for the on-axis hydrogens are given in Table 2. The positive charge is distributed over the molecule such that the (QTAIM) on-axis hydrogen charge increases to $+0.136e$. This causes a large increase in the charge contribution to the APT tensor element, which accounts for about 50% of the total change. The rest of the change is associated with the increased charge flux term which nearly doubles upon ionization. Again, the terms for the hydrogen and the carbon are in opposition, but that of the hydrogen increases, while that of the carbon atom decreases slightly. Again, the carbon gains more electron density than the hydrogen loses but the overall difference is between two large contributions, meaning that small changes in these can bring about large changes to the overall dipole moment. The associated dipole moment change on the carbon is very similar to the neutral, as is the total *DF* contribution. The major contributors to the difference upon ionization are the charge and the charge flux. The result is to "flip" the sign of the APT element from negative in the neutral to positive in the cation.

TABLE 3: Numerical QTAIM Decomposition of the APT Elements for the C−H Stretches of Naphthalene (Units in D/Å)

		neutral	cation	Δ
H1	$C_{\parallel}$	+0.179	+0.553	+0.374
□	$CF_{\parallel}$	+0.863	+1.237	+0.374
	$DF_{\parallel}$	−1.579	−1.596	−0.017
	total	−0.538	+0.193	+0.731
H2	$C_{\parallel}$	+0.191	+0.577	+0.386
○	$CF_{\parallel}$	+0.657	+1.212	+0.555
	$DF_{\parallel}$	−1.501	−1.586	−0.085
	total	−0.653	+0.204	+0.857

The off-axis hydrogens in the cation possess contributions to the induced dipole moment which are not parallel to their bond displacements. As such, the analysis is more complex. The overall dipole moment derivative for the bond elongation is 0.43 D/Å at an angle of about 41° from the hydrogen displacement vector. The charge component is large for the off-axis hydrogen, 0.737 D/Å, which accounts for nearly all the difference in the two positions. However, the QTAIM charge flux and dipole flux terms are 2.314 and 2.815 D/Å, roughly in opposition. The difference in these terms between the two hydrogen positions highlights that comparison of flux terms between dissimilar sites is difficult. A decomposition in terms parallel and perpendicular to the hydrogen displacement yield a $CF_{\parallel} = 1.980$ and $DF_{\parallel} = -2.392$ D/Å, which are still larger than those for the on-axis hydrogen. Nevertheless, it appears that half of the difference in the dipole moment derivative for C−H stretching of benzene, upon ionization, is accounted for by the charge difference, while the rest of the difference is accounted for in terms of flux.

Naphthalene. Naphthalene neutral has two inequivalent hydrogen positions, adjoining carbon atoms 1 and 2 in the IUPAC scheme. We refer to these as H1 and H2, respectively. QTAIM analysis of their APT elements for C−H bond elongation reveals that for the neutral and the cation the induced dipole moments are nearly (anti)parallel to the hydrogen displacements. For simplicity, therefore, we list only the parallel terms in Table 3.

Overall, the decomposition of the neutral naphthalene gives a very similar picture to that of benzene. The charge and charge flux are positive contributions while the dipole flux overcomes both of these to bring about a negative dipole derivative. In the case of both hydrogen positions, the difference between the neutral and the cation is about half due to the charge and about half due to the charge flux. However, as the charge is decreased, due to the greater delocalization in the larger naphthalene cation as compared to the benzene, the dipole derivatives for naphthalene cations are, in the end, only about half those of benzene.

TABLE 4: Numerical QTAIM Decomposition of the APT elements for the C−H Stretches of Pyrene (Units in D/Å)

		neutral	cation	Δ
H1	$C_{\|\|}$	+0.197	+0.487	+0.290
□	$CF_{\|\|}$	+0.502	+1.072	+0.570
	$DF_{\|\|}$	−1.489	−1.568	−0.079
	total	−0.790	−0.010	+0.780
H2	$C_{\|\|}$	+0.182	+0.477	+0.295
○	$CF_{\|\|}$	+0.791	+1.154	+0.363
	$DF_{\|\|}$	−1.576	−1.611	−0.035
	total	−0.603	+0.020	+0.623
H3	$C_{\|\|}$	+0.191	+0.464	+0.273
Δ	$CF_{\|\|}$	+0.762	+1.132	+0.370
	$DF_{\|\|}$	−1.550	−1.597	−0.047
	total	−0.596	−0.002	+0.594

TABLE 5: Numerical QTAIM Decomposition of the APT Elements for the C−H Stretches of ovalene (Units in D/Å)

		neutral	cation	Δ
H1	$C_{\|\|}$	+0.177	+0.381	+0.204
□	$CF_{\|\|}$	+0.814	+1.007	+0.193
	$DF_{\|\|}$	−1.593	−1.603	−0.010
	total	−0.602	−0.216	+0.386
H2	$C_{\|\|}$	+0.197	+0.374	+0.177
○	$CF_{\|\|}$	+0.676	+1.030	+0.354
	$DF_{\|\|}$	−1.548	−1.531	+0.017
	total	−0.676	−0.126	+0.550
H3	$C_{\|\|}$	+0.195	+0.376	+0.181
Δ	$CF_{\|\|}$	+0.582	+1.004	+0.422
	$DF_{\|\|}$	−1.537	−1.553	−0.016
	total	−0.760	−0.174	+0.586
H4	$C_{\|\|}$	+0.191	+0.372	+0.181
∇	$CF_{\|\|}$	+0.609	+0.991	+0.382
	$DF_{\|\|}$	−1.552	−1.553	−0.001
	total	−0.753	−0.190	+0.563

As a result, the C−H stretches of naphthalene cation will have only about 25% of the intensity of those of benzene.

Pyrene and Ovalene. Pyrene has three inequivalent hydrogen sites. These are labeled sequentially H1 (on axis), H2, and H3 in Table 4. We see that the neutral pyrenes behave in a similar way to naphthalene and benzene. Indeed, the positions that are most similar (H2 in naphthalene and H3 in pyrene; H1 in naphthalene and H in benzene) have similar charges. Upon ionization there is a continued diminution of the charge and charge flux contributions on going from naphthalene to pyrene. Indeed, this is such that the total dipole moment changes for pyrene cation hover around zero which means that the pyrene cation C−H stretches will be very weak indeed.

Ovalene has four inequivalent hydrogen sites. These are labeled sequentially H1 (on axis), H2, H3, and H4 in Table 5. In ovalene we see a logical extension of the effects of increasing size. The charge and charge flux contributions are smaller than those in pyrene while, in general, the dipole flux terms are roughly constant with size and do not change much upon ionization. The APT elements for the C−H stretches of ovalene are all negative, like the neutrals. This implies that the weakest C−H stretches of PAH cations occur for those in the size range near pyrene.

Discussion

Size Dependence of the C−H Stretching Mode Intensity. In Figure 1 the size dependencies of the dipole moment derivatives along the C−H coordinate for all unique hydrogens in the studied PAHs are reported. It is seen that the neutrals do not show any general size dependence and all exhibit a negative

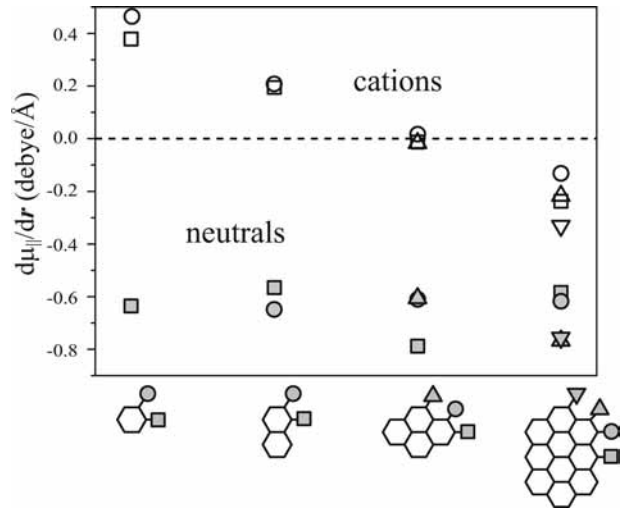

Figure 1. The dipole moment derivative with respect to the C−H stretching coordinate as a function of size of the PAHs.

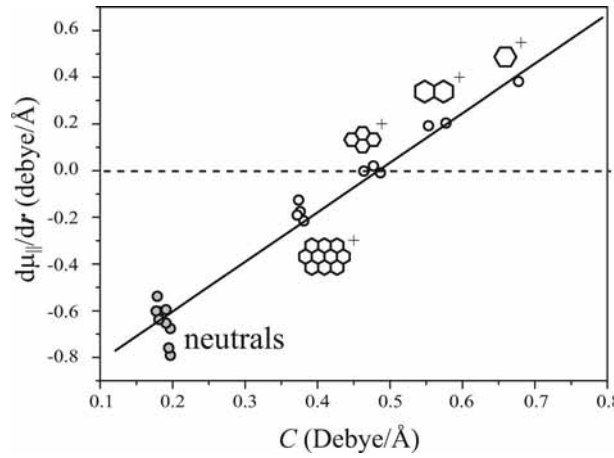

Figure 2. The dipole moment derivative with respect to the C−H stretching coordinate as a function of the charge contribution, *C* (see text for details).

value close to that in the benzene molecule. In the cations, the situation is completely different, a change in sign is observed and a slow convergence toward the value of the neutral with increasing size is observed. Because of the change of sign, the C−H dipole moment derivative passes through zero at a size close to that of pyrene and, therefore, infrared intensities are very weak for these intermediate sizes. In Figure 2, the dipole moment derivatives along the C−H coordinate for all different hydrogens in the studied PAHs are reported as a function of the charge contributions *C*. Upon ionization, the effective positive charge on the hydrogen is increased. With increasing size of the cation, a dilution of charge results in a convergence toward the *C* value of the neutral, all being similar to that of benzene. The exact same trend is observed for the charge flux *CF*. From our results, it is expected that PAH cations larger than ovalene should recover C−H stretch intensities comparable to those of the neutral. Quantum chemical calculations on larger PAHs confirm such an evolution[30,32,33,50] where the C−H stretch intensities are greater than 50% of the neutral for sizes above circumovalene ($C_{66}H_{20}$).

Astrophysical Implications. The size dependence of the intrinsic C−H stretching mode intensities in the PAH cations has not yet been properly taken into account in the various models of PAHs in the interstellar medium. In fact, the charge has been mainly considered to have just two effects: a collapse

of the C−H stretch intensity and a strong increase of the C−C stretch and in-plane >C−H bending modes. We have shown that a smooth size dependence for the compact PAHs is present, where PAHs above ovalene (32 carbon atoms) should recover some non-negligible C−H stretch intensities, typically for PAHs containing more than 60 carbon atoms. The carriers of the AIBs are predicted to have a size distribution peaking around 60 carbon atoms, extending up to a few hundred carbon atoms,[11,12,51] by considering details of the transient heating mechanism. Thus, it is clear that taking into account the size dependence of the C−H emission intensity should change the prediction of the size distribution and the relative weight of the neutral and cations. In particular, the contributions of the cations to the 3.3 μm bands should be reconsidered. Recently the emission spectrum using the theoretical emission spectra was modeled[34] and the ratio between the 3.3 and 11.3 μm bands was found to be similar for the PAHs containing 40−94 carbon atoms, being about 3 for the neutral and about 4 for the cations. It is thus clear that the model should include the intrinsic size dependence of the C−H stretches in order to properly model the balance between the charge and size of the interstellar PAHs that give rise to the AIBs.

Conclusion

The ionization effect on the C−H stretching mode intensities was investigated for standard PAHs. In order to disentangle the role of the positive charge dilution within the carbon skeleton and the peripheral hydrogens, the quantum theory of atoms in molecules was employed. The decomposition allowed the size evolution of the dipole moment derivative along the C−H stretch to be analyzed from benzene to ovalene, in their neutral and cationic forms. A clear collapse of the intensity of this mode was found for sizes around pyrene. However, this mode was found to recover intensity comparable to that of the neutral for sizes above ∼60 carbon atoms. Most observational studies of the aromatic infrared bands rely on the intensity ratio between the 7.7 and 11.3 μm bands to probe the charge state of the carriers, and up to now the ionization effect for these bands for isolated PAH seems reliable. However these models should consider the 3.3 μm band, the size dependence of which has not yet been included: The only effect of ionization generally considered is a decrease in intensity for the cations. In the future, infrared absorption (emission) cross sections for PAHs in the interstellar medium should include the intrinsic size dependence in order to properly model the infrared radiative cooling of the cations.

Acknowledgment. The authors wish to thank the CNRS for giving T.W.S. a visiting fellowship at the Laboratoire de Photophysique Moléculaire. This work has been supported by the French national program "Physique et Chimie du Milieu Interstellaire" and the French "Agence Nationale de la Recherche" (Contract ANR-05-BLAN-0148-02). This research was supported under the Australian Research Council's Discovery funding scheme (project numbers DP0665831 (T.W.S.)). T.W.S. and T.P. acknowledge helpful discussions with George Bacskay and Pascal Parneix, respectively.

References and Notes

(1) Désert, F.-X.; Boulanger, F.; Puget, J. L. *Astron. Astrophys.* **1990**, *237*, 215–236.
(2) Léger, A.; Puget, J. *Astron. Astrophys.* **1984**, *137*, L5.
(3) Allamandola, L. J.; Tielens, G. G. M.; Barker, J. R. *Astrophys. J., Suppl. Ser.* **1989**, *71*, 733–775.
(4) Gillett, F. C.; Forrest, W. J.; Merrill, K. M. *Astrophys. J.* **1973**, *183*, 87.
(5) Schutte, W.; Tielens, A.; Allamandola, L. *Astrophys. J.* **1993**, *415*, 397–414.
(6) Allamandola, L. J.; Bregman, J. D.; Sandford, S. A.; Tielens, A. G. G. M.; Witteborn, F. C.; Wooden, D. H.; Rank, D. *Astrophys. J. Lett.* **1989**, *345*, L59–L62.
(7) Moutou, C.; Verstraete, L.; Léger, A.; Sellgren, K.; Schmidt, W. *Astron. Astrophys.* **2000**, *354*, L17−L20.
(8) Duley, W. W.; Williams, D. A. *Mon. Not. R. Astron. Soc.* **1981**, *196*, 269–274.
(9) Peeters, E.; Hony, S.; van Kerckhoven, C.; Tielens, A. G. G. M.; Allamandola, L. J.; Hudgins, D. M.; Bauschlicher, C. W. *Astron. Astrophys.* **2002**, *390*, 1089.
(10) Galliano, F.; Madden, S. C.; Tielens, A. G. G. M.; Peeters, E.; Jones, A. P. ArXiv e-prints 2008, arXiv:0801.4955.
(11) Flagey, N.; Boulanger, F.; Verstraete, L.; Miville Deschenes, M. A.; Noriega Crespo, A.; Reach, W. T. *Astron. Astrophys.* **2006**, *453*, 969–978.
(12) Draine, B. T.; Li, A. *Astrophys. J.* **2007**, *657*, 810–837.
(13) van Diedenhoven, B.; E.Peeters,; van Kerckhoven, C.; Hony, S.; Hudgins, D. M.; Allamandola, L. J.; Tielens, A. G. G. M. *Astrophys. J.* **2004**, *611*, 928.
(14) Sloan, G. C.; Jura, M.; Duley, W. W.; Kraemer, K. E.; Bernard-Salas, J.; Forrest, W. J.; Sargent, B.; Li, A.; Barry, D. J.; Bohac, C. J.; Watson, D. M.; Houck, J. R. *Astrophys. J.* **2007**, *664*, 1144–1153.
(15) Pino, T.; Dartois, E.; Cao, A.-T.; Carpentier, Y.; Chamaillé, T.; Vasquez, R.; Jones, A. P.; D'Hendecourt, L.; Bréchignac, P. *Astron. Astrophys.* **2008**, *490*, 665–672.
(16) Verstraete, L.; Pech, C.; Moutou, C.; Sellgren, K.; Wright, C. M.; Giard, M.; Léger, A.; Timmermann, R.; Drapatz, S. *Astron. Astrophys.* **2001**, *372*, 981–997.
(17) Zubko, V.; Dwek, E.; Arendt, R. G. *Astrophys. J., Suppl. Ser.* **2004**, *152*, 211–249.
(18) Szczepanski, J.; Vala, M. *Nature (London)* **1993**, *363*, 699–701.
(19) Szczepanski, J.; Vala, M. *Astrophys. J.* **1993**, *414*, 646–655.
(20) D'Hendecourt, L. The PAH Hypothesis: Infrared Spectroscopic Properties of PAHs. *From Stardust to Planetesimals*; Astronomical Society of the Pacific: San Francisco, CA, 1997; p 129.
(21) Allamandola, L. J.; Hudgins, D. M.; Sandford, S. A. *Astrophys. J. Lett.* **1999**, *511*, L115–L119.
(22) Hudgins, D.; Bauschlicher, C.; Allamandola, L.; Fetzer, J. *J. Phys. Chem. A* **2000**, *104*, 3655–3669.
(23) de Frees, D. J.; Miller, M. D.; Talbi, D.; Pauzat, F.; Ellinger, Y. *Astrophys. J.* **1993**, *408*, 530–538.
(24) Langhoff, S. *J. Phys. Chem.* **1996**, *100*, 2819–2841.
(25) Pauzat, F.; Talbi, D.; Ellinger, Y. *Astron. Astrophys.* **1997**, *319*, 318–330.
(26) Bauschlicher, C. W., Jr. *Chem. Phys.* **1998**, *234*, 79–86.
(27) Pauzat, F.; Talbi, D.; Ellinger, Y. *Mon. Not. R. Astron. Soc.* **1999**, *304*, 241–253.
(28) Pauzat, F.; Ellinger, Y. *Mon. Not. R. Astron. Soc.* **2001**, *324*, 355–366.
(29) Bakes, E. L. O.; Tielens, A.; G, G. M.; Bauschlicher, C. W., Jr. *Astrophys. J.* **2001**, *556*, 501–514.
(30) Bauschlicher, C. W., Jr. *Astrophys. J.* **2002**, *564*, 782–786.
(31) Pathak, A.; Rastogi, S. *Chem. Phys.* **2005**, *313*, 133–150.
(32) Malloci, G.; Joblin, C.; Mulas, G. *Chem. Phys.* **2007**, *332*, 353–359.
(33) Bauschlicher, C. W., Jr.; Peeters, E.; Allamandola, L. J. *Astrophys. J.* **2008**, *678*, 316–327.
(34) Pathak, A.; Rastogi, S. *Astron. Astrophys.* **2008**, *485*, 735–742.
(35) Malloci, G.; Joblin, C.; Mulas, G. *Astron. Astrophys.* **2007**, *462*, 627–635.
(36) da Silva, J. V.; Faria, S. H. D. M.; Haiduke, R. L. A.; Bruns, R. E. *J. Phys. Chem. A* **2007**, *111*, 515–520.
(37) Faria, S. H. D. M.; da Silva, J. V.; Haiduke, R. L. A.; Vidal, L. N.; Vazquez, P. A. M.; Bruns, R. E. *J. Phys. Chem. A* **2007**, *111*, 7870–7875.
(38) da Silva, J. V.; Haiduke, R. L. A.; Bruns, R. E. *J. Phys. Chem. A* **2006**, *110*, 4839–4845.
(39) Haiduke, R. L. A.; Bruns, R. E. *J. Phys. Chem. A* **2005**, *109*, 2680.
(40) Bader, R. F. W. *J. Chem. Phys.* **1987**, *87*, 1142.
(41) Bader, R. F. W. *Chem. Rev.* **1991**, *91*, 893.
(42) Bader, R. F. W. *Atoms in Molecules: A Quantum Theory*; Clarendon Press: Oxford, 1990.
(43) Schmidt, M. W.; Baldridge, K. K.; Boatz, J. A.; Elbert, S. T.; Gordon, M. S.; Jensen, J. H.; Koseki, S.; Matsunaga, N.; Nguyen, K. A.; Su, S.; Windus, T. L.; Dupuis, M.; Montgomery, J. A. *J. Comput. Chem.* **1993**, *14*, 1347–1363.
(44) Gordon, M. S.; Schmidt, M. W. In *Advances in electronic structure theory: GAMESS a decade later*; Dykstra, C. E. Frenking, G. Kim, K. S. Scuseria, G. E., Eds.; Elsevier: Amsterdam, 2005; pp 1167−1189.
(45) Frisch, M. J.; Trucks, G. W.; Schlegel, H. B.; Scuseria, G. E.; Robb, M. A.; Cheeseman, J. R.; Montgomery, J. A., Jr.; Vreven, T.; Kudin, K. N.;

Burant, J. C.; Millam, J. M.; Iyengar, S. S.; Tomasi, J.; Barone, V.; Mennucci, B.; Cossi, M.; Scalmani, G.; Rega, N.; Petersson, G. A.; Nakatsuji, H.; Hada, M.; Ehara, M.; Toyota, K.; Fukuda, R.; Hasegawa, J.; Ishida, M.; Nakajima, T.; Honda, Y.; Kitao, O.; Nakai, H.; Klene, M.; Li, X.; Knox, J. E.; Hratchian, H. P.; Cross, J. B.; Adamo, C.; Jaramillo, J.; Gomperts, R.; Stratmann, R. E.; Yazyev, O.; Austin, A. J.; Cammi, R.; Pomelli, C.; Ochterski, J. W.; Ayala, P. Y.; Morokuma, K.; Voth, G. A.; Salvador, P.; Dannenberg, J. J.; Zakrzewski, V. G.; Dapprich, S.; Daniels, A. D.; Strain, M. C.; Farkas, O.; Malick, D. K.; Rabuck, A. D.; Raghavachari, K.; Foresman, J. B.; Ortiz, J. V.; Cui, Q.; Baboul, A. G.; Clifford, S.; Cioslowski, J.; Stefanov, B. B.; Liu, G.; Liashenko, A.; Piskorz, P.; Komaromi, I.; Martin, R. L.; Fox, D. J.; Keith, T.; Al-Laham, M. A.; Peng, C. Y.; Nanayakkara, A.; Challacombe, M.; Gill, P. M. W.; Johnson, B.; Chen, W.; Wong, M. W.; Gonzalez, C.; Pople, J. A. *Gaussian 03, Revision C.02*; Gaussian, Inc.: Wallingford, CT, 2004.

(46) Choi, C. H.; Kertesz, M. *Chem. Phys. Lett.* **1996**, *263*, 697–702.

(47) Gussoni, M.; Castiglioni, C. *J. Mol. Struct.* **2000**, *521*, 1–18.

(48) Gussoni, M.; Castiglioni, C.; Zerbi, G. *J. Phys. Chem.* **1984**, *88*, 600–604.

(49) Deleuze, M. S.; Claes, L.; Kryachko, E. S.; Francois, J.-P. *J. Chem. Phys.* **2003**, *119*, 3106–3119.

(50) Pathak, A.; Rastogi, S. *Spectrochim. Acta* **2007**, *67*, 898.

(51) Compiègne, M.; Abergel, A.; Verstraete, L.; Reach, W. T.; Habart, E.; Smith, J. D.; Boulanger, F.; Joblin, C. *Astron. Astrophys.* **2007**, *471*, 205–212.

JP900931E